

## Microphysical Interpretation of Multiparameter Radar Measurements in Rain. Part III: Interpretation and Measurement of Propagation Differential Phase Shift between Orthogonal Linear Polarizations

A. R. JAMESON

*Illinois State Water Survey, Champaign, IL 61820*

(Manuscript received 18 January 1984, in final form 18 December 1984)

### ABSTRACT

As radar waves having different polarizations propagate through a collection of nonspherical oriented hydrometeors, a phase difference between the waves appears. In a collection of uniformly horizontally oriented quiescent water drops, the rate of change of the propagation differential phase shift with increasing distance from the radar is proportional to the product of the liquid water content and the departure from unity of the mass-weighted mean axis ratio of the drops provided the radar wavelength is much larger than the drops. The appropriateness, however, of such a simple relation to natural rain in which some drops assume complex shapes and a variety of orientations through the processes of collision, coalescence, break-up and oscillation remains to be determined.

### 1. Introduction

The electromagnetic wave backscattered to a radar from hydrometeors provides information about the precipitation. At any instant this wave can be specified by an amplitude and a phase angle. Traditional radar parameters usually depend only on the amplitude of the backscattered signals. The natural complexity and diversity of precipitation, however, requires extracting as much information as possible from the signals. Consequently the phase component of the backscattered waves should also be used.

The wave returned to a radar can be decomposed into a component having the same polarization as the transmitted wave (co-polarized component) and another component "oppositely" polarized (cross-polarized or orthogonally<sup>1</sup> polarized component). The relative phase between these two components, which can be measured by radars capable of receiving the co- and cross-polarized components simultaneously, is determined by several factors including the polarization of the transmission, the characteristics of the backscattering hydrometeors and the nature and extent of the precipitation encountered during propagation.

As a radar wave passes through a region containing oriented nonspherical hydrometeors the wave incident

on scatterers at point P consists of a component due to the transmitted wave plus another component due to forward scattering by hydrometeors upstream of P (van de Hulst, 1957). Because of the different origins of these two waves, the phase angles of each component will be different. When the forward scattered wave is added to the transmitted wave, the phase angle of the net electric field vector will differ from that of the transmitted component alone. This phase difference may be called the propagation phase shift.

Since the forward scattered component depends upon the polarization of the transmitted wave, the propagation phase shift will vary for different polarizations. The inequalities between propagation phase shifts corresponding to different transmission polarizations may be called the propagation differential phase shifts.

Because all elliptical polarizations can be expressed as a linear combination of vertically and horizontally linearly polarized components, only the horizontal-vertical linear polarization pair will be considered further. Propagation differential phase shift henceforth will refer exclusively to this polarization couplet.

Propagation differential phase shifts can become substantial in rain (e.g., Humphries, 1974) and, in many situations, can dominate the relative phase between the horizontally and vertically polarized components of the backscattered wave. Determining which meteorological quantities significantly influence the propagation differential phase shift in rain, however, is not trivial. Within rain, quiescent, horizontally oriented approximately oblate drops may co-exist

<sup>1</sup> Mathematically, the transmitted and orthogonally polarized electric fields can be considered elements of two different complex vector spaces each spanned by a different unit basis vector such that the dot product between them is zero. Right- and left-hand circular polarizations as well as vertical and horizontal linear polarizations are frequently used orthogonal pairs.

with others having complex shapes and a variety of orientations as a consequence of drop collisions, coalescence, breakup, and oscillation. However, because so little is known about the impact of these processes on the shapes and orientations of the drops, a complete theoretical treatment incorporating all of this natural complexity can not yet be formulated. Rain, though, is highly oriented (McCormick *et al.*, 1972; McCormick and Hendry, 1974; Beard and Jameson, 1983; Hendry and Antar, 1984). If a major fraction of the drops were greatly perturbed, rain would not exhibit such pervasive orientation. To a first approximation, therefore, rain can be represented by a collection of uniformly oriented oblate quiescent water drops. This simplification has often been used in theoretical investigations of electromagnetic scattering by rain.

## 2. Meteorological factors which influence the propagation differential phase shift in rain

For a single particle the relation between the scattered and incident waves may be expressed by a complex amplitude function ( $S$ ) which depends on the particle characteristics and the relative angles of the incident wave and viewing angle of an observer with respect to the particle.

For an ensemble of particles which scatter independently of one another and which occupy a region of incremental length  $\delta R$  along the direction of a radar transmission, the two-way propagation induced phase change of the radar wave which first traverses and, upon backscattering, returns through the region of particles is given by (after van de Hulst, 1957),

$$\Delta\Phi = 2\delta Rk \left[ \frac{2\pi}{k^2} \int \text{Re}(S_0)_D N_D dD \right], \quad (1)$$

where  $N_D dD$  is the number of drops per unit volume of diameter  $D$  to  $D + dD$ . In (1)  $k$  is the wave number ( $2\pi/\lambda$ ) where  $\lambda$  is the radar wavelength,  $S_0$  denotes the forward scattered amplitude function using the convention of Warner and Hizal (1976),  $\text{Re}$  denotes the real part of  $S_0$ , and the integral is over the drop size distribution in the volume of the radar beams having uniform illumination. The one-way range rate of propagation differential phase shift between horizontally ( $H$ ) and vertically ( $V$ ) polarized waves over the distance is then given by

$$\Phi_{HV} = \frac{2\pi}{k} \int \{ [\text{Re}(S_0)_D]_H - [\text{Re}(S_0)_D]_V \} N_D dD. \quad (2)$$

For oblate shaped water drops,  $S_0$  is a function of the equivalent volume drop diameter and the axis ratio. The backscatter cross-section (which is proportional to  $|S_\pi|^2$  where  $\pi$  denotes backscatter) of an oblate water drop is well described by Rayleigh-Gans theory for radar wavelengths much larger than the drops. Under that restriction the influences of size

and of axis ratio on  $S_\pi$  are separable. Similarly,  $S_0$  may be separated. For horizontal and vertical linear polarizations, values of  $S_0$  were computed using a program provided by C. Warner (personal communication, 1978) which is based on the method of Warner and Hizal (1976). At both polarizations  $S_0$  was found to be proportional to  $D^3$  times a polarization dependent axis ratio term. More specifically to a good approximation (correlation coefficient of 0.998; see Fig. 1)

$$\text{Re}(S_0)_H - \text{Re}(S_0)_V = D^3 C(1 - r), \quad (3)$$

where  $r$  is the oblate drop axis ratio and  $C = 0.5987$  and  $0.05717$  at wavelengths of 3.21 and 10.71 cm, respectively.

From (2) and (3) it follows that

$$\Phi_{HV} = \frac{2\pi}{k} \int D^3 C(1 - r) N_D dD \quad (4a)$$

$$= \frac{108}{\pi^2} W \lambda C [1 - \mathfrak{A}], \quad (4b)$$

where  $W$  is the liquid water content in  $\text{g m}^{-3}$ ,  $\lambda$  is the radar wavelength in cm,  $\Phi_{HV}$  is the one-way differential phase shift rate in degrees  $\text{km}^{-1}$  and  $\mathfrak{A}$  is the mass weighted mean axis ratio defined by

$$\mathfrak{A} = \frac{\int D^3 r N_D dD}{\int D^3 N_D dD}. \quad (5)$$

While the dependence of  $\Phi_{HV}$  on the deviation of drop axis ratio from unity is not surprising, the origin of the dependence on  $W$  is less obvious. Recalling that for a single drop  $S_0$  is proportional to  $D^3$  times a shape term, then for an ensemble of oblate water drops it is easy to show that the magnitude of the forward scattered wave ( $|E_f|_{H,V}$ ) is proportional to  $W$  times a mean shape factor which will be different for horizontal and vertical polarizations. If  $W$  is increased by a factor  $F$ ,  $|E_f|_H$  and  $|E_f|_V$  both increase by the same factor but  $|E_f|_H$  will always be greater than  $|E_f|_V$  because of the difference between the mean shape terms. Consequently an increase by  $F$  in the forward scattered component which is then added to the transmitted wave produces a greater increase in the propagation phase shift  $\phi_H$  than in  $\phi_V$ . Hence, over an incremental distance  $\delta R$ ,  $\Phi_{HV}$  also increases with increasing  $W$ .

For oblate quiescent water drops, (4b) suggests that if  $\Phi_{HV}$  and  $\mathfrak{A}$  were known then  $W$  could be determined without any assumptions about the form or size limits of the drop size distribution provided  $\mathfrak{A}$ , which is defined mathematically by (5), is physically real. [For a bimodal drop shape distribution, for example,  $\mathfrak{A}$  may be calculated using (5), but none of the drops may actually possess an axis ratio equal to  $\mathfrak{A}$ . In that case  $\mathfrak{A}$  would have no physical meaning.] In the next

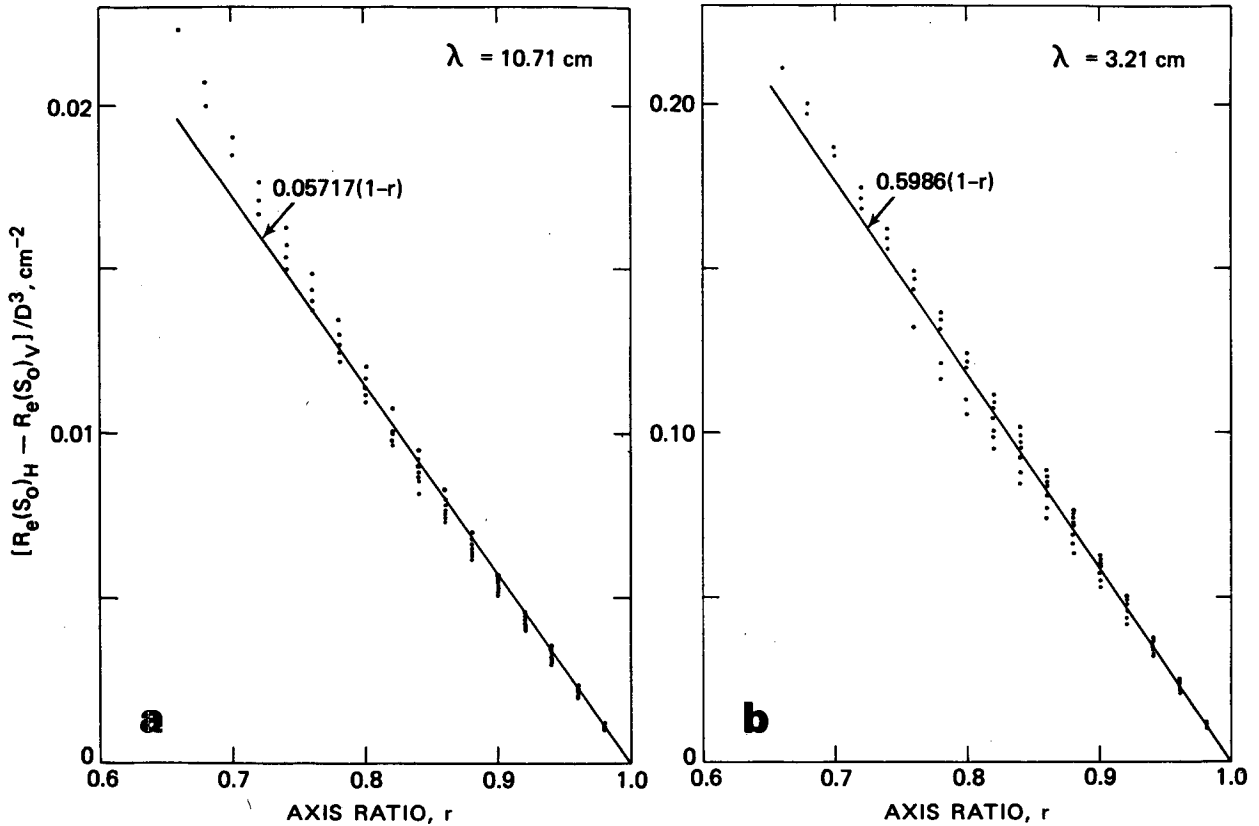


FIG. 1. Linear fit of  $\{Re(S_{0H}) - Re(S_{0V})\}$  normalized by  $D^3$  to raindrop axis ratio at 10.71 cm (a) and 3.21 cm (b) radar wavelengths for drops 0.15–0.6 cm diameter and  $r$  ranging from unity to the equilibrium value (Pruppacher and Pitter, 1971) appropriate to each drop size.

two sections methods for estimating both  $\mathcal{R}$  and  $\Phi_{HV}$  are discussed.

**3. Estimation of  $\mathcal{R}$  from polarization measurements**

Although conventional polarization measurements can be used to estimate the reflectivity weighted mean axis ratio ( $\mathcal{R}$ ) (Jameson, 1983a), such measurements do not yield a direct measure of  $\mathcal{R}$ . For many size distributions of quiescent, horizontally oriented drops, however,  $\mathcal{R}$  is closely related to  $\mathcal{R}$  and the standard deviation ( $\sigma_{\mathcal{R}}$ ) of the axis ratio distribution.

This relationship can be made more explicit using a generalized form of drop size distributions. From an analysis of drop size distributions observed in a wide variety of meteorological conditions Ulbrich (1983) proposed the following general formula:

$$N_D dD = N_0 D^n e^{-\Lambda D}, \tag{6}$$

where  $-2 \leq n \leq 3$  corresponds to different particular forms of distributions (e.g., exponential, gamma, etc.). If in a distribution drop sizes are considered to extend from 0 to  $\infty$  (infinite distributions) then direct integration of (6) for the reflectivity weighted (approximately  $D^6$ ) mean drop diameter  $\mathcal{D}$ , the variance of  $\mathcal{D}$  ( $\sigma_{\mathcal{D}}^2$ ), and the mass weighted mean drop diameter  $\bar{D}$  are given by

$$\mathcal{D} = \frac{\int_0^\infty N_0 D^{7+n} e^{-\Lambda D} dD}{\int_0^\infty N_0 D^{6+n} e^{-\Lambda D} dD} = \frac{n+7}{\Lambda}, \tag{7}$$

$$\sigma_{\mathcal{D}}^2 = \frac{\int_0^\infty N_0 D^{8+n} e^{-\Lambda D} dD}{\int_0^\infty N_0 D^{6+n} e^{-\Lambda D} dD} - \mathcal{D}^2 = \frac{n+7}{\Lambda^2}, \tag{8}$$

$$\bar{D} = \frac{\int_0^\infty N_0 D^{4+n} e^{-\Lambda D} dD}{\int_0^\infty N_0 D^{3+n} e^{-\Lambda D} dD} = \frac{n+4}{\Lambda}. \tag{9}$$

Observations of rain drops near the ground and of water drops in wind tunnels suggest that to a good approximation the relation between drop diameter and axis ratio is approximately linear, i.e.,  $r = a - bD$  (Jameson, 1983b). Using this relationship, (8) can be rewritten as

$$\sigma_{\mathcal{R}}^2 = \frac{b^2(n+7)}{\Lambda^2}. \tag{10}$$

It is also true then that

$$\mathcal{Y} - \mathcal{R} = b(\mathcal{D} - \bar{\mathcal{D}}) \quad (11a)$$

$$= b \frac{3}{\Lambda}. \quad (11b)$$

From (10) and (11b) it follows that

$$\mathcal{Y} = \mathcal{R} + F\sigma_{\mathcal{R}}^{\infty}, \quad (12)$$

where  $F = 3/(n+7)^{0.5}$  and  $\infty$  denotes an infinite distribution. For the exponential ( $n=0$ ) and gamma ( $n=1-3$ ) drop size distributions, for example,  $F$  is 1.13 and 1.06–0.95, respectively.

The assumption of an infinite drop size distribution, however, is of limited value since through the physical processes of drop breakup, size sorting due to wind shear and the differential fall speeds of different sized drops many natural drop distributions will often be truncated. To account for truncation it should be noted that when the limits of integration in (7)–(9) are replaced by the maximum ( $D_{\max}$ ) and minimum ( $D_{\min}$ ) drop diameters then

$$\mathcal{D} = \frac{f_{n7}}{f_{n6}} \left( \frac{n+7}{\Lambda} \right), \quad (13)$$

$$\sigma_{\mathcal{D}}^2 = \left[ \frac{f_{n8}(n+8)!}{f_{n6}(n+6)!} - \frac{f_{n7}^2}{f_{n6}^2} (n+7)^2 \right] / \Lambda^2, \quad (14)$$

$$\bar{\mathcal{D}} = \frac{f_{n4}}{f_{n3}} \left( \frac{n+4}{\Lambda} \right), \quad (15)$$

where  $f_{nm}$  is the incomplete gamma function appropriate for  $D^m$  and is defined by

$$f_{nm} = \frac{\int_{D_{\min}}^{D_{\max}} D^{n+m} e^{-\Lambda D} dD}{\int_0^{\infty} D^{n+m} e^{-\Lambda D} dD}. \quad (16)$$

The integer  $n$  is identical to that in (6). As in the derivation of (12) it follows that

$$\begin{aligned} \mathcal{Y} - \mathcal{R} &= F\sigma_{\mathcal{R}}^{\infty} \frac{n(f_{n3}f_{n7} - f_{n4}f_{n6}) + 7f_{n3}f_{n7} - 4f_{n4}f_{n6}}{3f_{n3}[n(f_{n8}f_{n6} - f_{n7}^2) + 8f_{n8}f_{n6} - 7f_{n7}^2]^{0.5}}, \end{aligned} \quad (17)$$

or in terms of  $\sigma_{\mathcal{R}}$  of the truncated distribution

$$\begin{aligned} \mathcal{Y} - \mathcal{R} &= \sigma_{\mathcal{R}} F f_{n6} [n(f_{n3}f_{n6} - f_{n4}f_{n6}) \\ &\quad + 7f_{n3}f_{n7} - 4f_{n4}f_{n6}] / 3. \end{aligned} \quad (18)$$

For an ensemble of quiescent horizontally oriented oblate drops  $\mathcal{R}$  can be determined (Jameson, 1983a) from measurements of the differential reflectivity (Seliga and Bringi, 1976) while  $\sigma_{\mathcal{R}}$  can be deduced (Jameson, 1983a) using 'pseudo-circular' parameters derivable from linear polarization measurements in

which the effects of propagation differential phase shift have been eliminated (Jameson and Mueller, 1985). The quantities  $n$ ,  $F$ ,  $f_{n3}$ ,  $f_{n4}$ ,  $f_{n6}$ ,  $f_{n7}$ , however, remain unknown.

The variability these unknowns introduce into the estimation of  $\mathcal{Y}$  from  $\mathcal{R}$  and  $\sigma_{\mathcal{R}}$  can be investigated numerically. Calculations were made for Gaussian-like, gamma, and exponential distributions with  $\Lambda$  from 0.1 to 40  $\text{cm}^{-1}$  ( $\text{cm}^{-2}$  for the Gaussian distribution). The  $D_{\max}$  was varied from 0.1 to 0.6 cm while  $D_{\min}$  was varied from 0.01 to  $D_{\max}$ .

The values of  $\mathcal{Y} - \mathcal{R}$  as a function of  $\sigma_{\mathcal{R}}$  for these drop size distributions are contained within the shaded area in Fig. 2. The frequencies of occurrence for all the drop distributions were equal. The solid line in Fig. 2a is a least square error power law fit given by

$$\mathcal{Y} - \mathcal{R} = 5.133\sigma_{\mathcal{R}}^{1.506} \quad (19)$$

with a correlation coefficient of 0.89. Although the scatter about (19) can approach  $\pm 0.022$  the root-mean-square deviation is only 0.006. Nearly 90% of all the model drop size distribution values lie within  $\pm 0.01$  of (19).

Much of the scatter apparent in Fig. 2a is produced by drop size distributions with a minimum diameter in excess of 0.1 cm. Because of the large volumes ( $10^8$ – $10^9 \text{m}^3$ ) usually sampled by radar, it may often be reasonable to assume that the minimum diameter  $\leq 0.1$  cm. Under this restriction the scatter is significantly reduced (Fig. 2b). This is reflected by an increase in the correlation coefficient to 0.95 for the fit given by

$$\mathcal{Y} - \mathcal{R} = 1.949\sigma_{\mathcal{R}}^{1.172}. \quad (20)$$

The root-mean-square deviation from (20) is 0.004. Although the maximum scatter is  $\pm 0.016$ , 90% of all values lie within  $\pm 0.007$  of (20).

#### 4. Estimating the propagation differential phase shift at linear polarizations

In order to estimate  $\Phi_{HV}$  it is necessary, of course, to measure the propagation phase shifts at both horizontal and vertical polarizations as functions of radar range. Meteorological radars usually transmit periodic bursts of energy. During the interval between bursts while the radar measures backscattered waves the scatterers move relative to each other and the radar. Consequently measurements of the phase show considerable variation during a sequence of pulses. Although this time variation in the phase ultimately leads to estimates of important quantities such as the mean Doppler velocity, the effect of particle motion must be taken into account before estimating  $\phi_H$  and  $\phi_V$ .

Although the wave backscattered to the radar from hydrometeors usually consists of a horizontally and a vertically polarized component, many radars receive

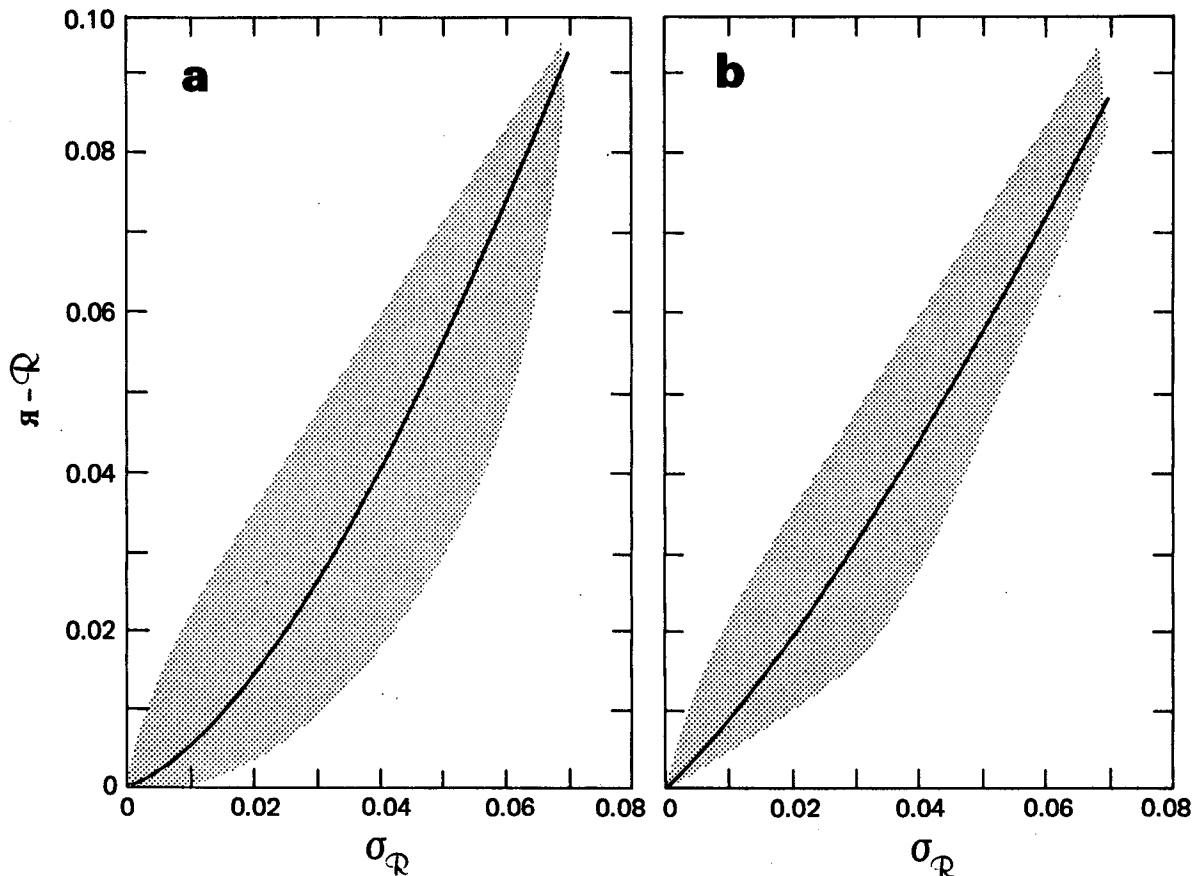


FIG. 2. The difference between the mass-weighted mean axis ratio  $\mathcal{A}$  and the reflectivity-weighted mean axis ratio  $\mathcal{R}$  vs the standard deviation of the axis ratio distribution for (a) the minimum drop diameter ( $D_{\min}$ ) between 0.01 to 0.6 cm and for (b)  $D_{\min} \leq 0.1$  cm. These results apply to quiescent drops for several different types of drop size distributions. The shaded region encloses all computed values. Most values lie much closer to the best fit solid lines than implied by the shading (see text).

only one (the co-polarized) component at a time. The polarization of the transmission and receiver are then switched to gather measurements at the orthogonal co-polarization. If the sequence of measurements is made properly the effect of particle motion on the phases measured at the different times can be removed, and  $\phi_H - \phi_V$  can then be estimated (Jameson and Mueller, 1985).

Alternatively, if a radar is equipped to measure simultaneously both the co- and cross-polarized components, particle motion no longer affects the relative phase between the two signals. In this section it will be shown that, in principle,  $\phi_H - \phi_V$  can then be readily estimated.

A cross-polarized signal, however, will only be produced when the hydrometeors are asymmetric or are symmetric but canted. The wave backscattered from a collection of uniformly horizontally oriented, quiescent drops would be purely co-polarized so that the method of Jameson and Mueller for example, would have to be used to measure  $\phi_H - \phi_V$ . On the other hand in rain, collisions (e.g., Johnson and

Beard, 1984) will often produce some asymmetric drops and some canted symmetric drops. The resulting cross-polarized component originating from these drops can be measured in rain and appears to be about 30 dB below the intensity of the co-polarized component (Hendry and Antar, 1984). It is worthwhile, therefore, to pursue the estimation of  $\phi_H - \phi_V$  using simultaneous measurements of the co- and cross-polarized signals even in a highly oriented medium such as rain.

Suppose a radar alternately transmits horizontally and vertically polarized signals every millisecond and simultaneously receives the co- and cross-polarized signals. Following a transmission at horizontal polarization, the signals are given by

$$\left. \begin{aligned} E_{HH} &= \sum_i |S_{HH}|^i \exp[j(\gamma_i + \delta_{HH}^i + 2\phi_H^i)] \\ E_{HV} &= \sum_i |S_{HV}|^i \exp[j(\gamma_i + \delta_{HV}^i + \phi_H^i + \phi_V^i)] \end{aligned} \right\} \quad (21a)$$

while after a vertically polarized transmission

$$\left. \begin{aligned} E_{VV} &= \sum_i |S_{VV}^i|^2 \exp[j(\gamma_i + \delta_{VV}^i + 2\phi_V^i)] \\ E_{VH} &= \sum_i |S_{VH}^i|^2 \exp[j(\gamma_i + \delta_{VH}^i + \phi_V^i + \phi_H^i)] \end{aligned} \right\}, \quad (21b)$$

where  $E_{HH}$ ,  $E_{HV}$ ,  $E_{VV}$ , and  $E_{VH}$  have been normalized by the transmitted field at the range of the uniformly illuminated pulse volume, the summation is over the particles in the pulse volume,  $j = \sqrt{-1}$ , and  $|S_{ir}^i|^2 \exp[j\delta_{ir}^i]$  are the backscatter matrix elements (Sinclair, 1948) of each particle corresponding to the polarizations of the transmitted ( $t$ ) and received ( $r$ ) signals. The propagation phase shifts ( $\phi_H^i$ ,  $\phi_V^i$ ) as well as the random phase positions ( $\gamma_i$ ) are functions of  $R_i$ , the distance between a scatterer and the radar. In particular  $\gamma_i = 4\pi R_i/\lambda$  where  $\lambda$  is the radar wavelength.

Using (21) two products can be formed, i.e.,

$$E_{HV}E_{HH}^* = \sum_i \sum_l |S_{HV}^i|^2 |S_{HH}^l|^2 \exp\left\{j\left[\delta_{HV}^i - \delta_{HH}^l + \phi_V^i - \phi_H^l + \frac{4\pi}{\lambda}(R_i - R_l)\right]\right\}, \quad (22a)$$

$$E_{VH}E_{VV}^* = \sum_i \sum_l |S_{VH}^i|^2 |S_{VV}^l|^2 \exp\left\{j\left[\delta_{VH}^i - \delta_{VV}^l + \phi_H^i - \phi_V^l + \frac{4\pi}{\lambda}(R_i - R_l)\right]\right\}, \quad (22b)$$

where the asterisk denotes complex conjugate. Since particle position is independent of the physical properties of the scatterers it is appropriate to take the ensemble average over  $R$ . Remembering that  $\phi_H^i$  and  $\phi_V^i$  are functions of radar range, the ensemble averages of (22) become

$$\langle E_{HV}E_{HH}^* \rangle \approx \exp[j(\phi_V - \phi_H)] \sum_i |S_{HV}^i|^2 |S_{HH}^i|^2 \times \exp[j(\delta_{HV}^i - \delta_{HH}^i)], \quad (23a)$$

$$\langle E_{VH}E_{VV}^* \rangle \approx \exp[j(\phi_H - \phi_V)] \sum_i |S_{VH}^i|^2 |S_{VV}^i|^2 \times \exp[j(\delta_{VH}^i - \delta_{VV}^i)], \quad (23b)$$

where it has been assumed that the depth of the sampling volume is sufficiently small so that  $(\phi_H^i - \phi_V^i)$  are narrowly distributed about  $(\phi_H - \phi_V)$  at the center of the sampling volume, and that  $\gamma_i$  and  $\gamma_l$  are distributed uniformly over  $2\pi$ .

A useful simplification of (23) is possible. For Rayleigh-Gans scatterers  $\delta_{HH}$ ,  $\delta_{VV}$ ,  $\delta_{HV}$ , and  $\delta_{VH}$  are small and

$$\begin{aligned} &\sum_i |S_{HV}^i|^2 |S_{HH}^i|^2 \exp\{j(\delta_{HV}^i - \delta_{HH}^i)\} \\ &\approx \sum_i |S_{HV}^i|^2 |S_{HH}^i|^2 \{1 + j(\delta_{HV}^i - \delta_{HH}^i)\} \end{aligned} \quad (24a)$$

$$\approx \{1 + j(\overline{\delta_{HV}} - \overline{\delta_{HH}})\} \sum_i |S_{HV}^i|^2 |S_{HH}^i|^2 \quad (24b)$$

$$\approx \exp\{j(\overline{\delta_{HV}} - \overline{\delta_{HH}})\} \sum_i |S_{HV}^i|^2 |S_{HH}^i|^2, \quad (24c)$$

where, for example, the overbar denotes averaging like

$$\overline{\delta_{HV}} = \frac{\sum_i |S_{HV}^i|^2 |S_{HH}^i|^2 \delta_{HV}^i}{\sum_i |S_{HV}^i|^2 |S_{HH}^i|^2}. \quad (25)$$

Expression (23) then becomes

$$\langle E_{HV}E_{HH}^* \rangle \approx \exp[j(\phi_V - \phi_H + \overline{\delta_{HV}} - \overline{\delta_{HH}})] \times \sum_i |S_{HV}^i|^2 |S_{HH}^i|^2 \quad (26a)$$

$$\langle E_{VH}E_{VV}^* \rangle \approx \exp[j(\phi_H - \phi_V + \overline{\delta_{VH}} - \overline{\delta_{VV}})] \times \sum_i |S_{VH}^i|^2 |S_{VV}^i|^2. \quad (26b)$$

[Actually (26) applies to non-Rayleigh-Gans scatterers as well but the physical interpretation of terms like  $\delta_{HV}$  is not as direct as in (25).] Under the usual assumption of ergodicity (26) can be evaluated from a time series provided the distributions of  $|S_{ir}^i|^2 \exp[j\delta_{ir}^i]$  do not change substantially during the observation interval.

The ratio of the quantities in (26) then becomes

$$\begin{aligned} \mu &= \frac{\langle E_{VH}E_{VV}^* \rangle}{\langle E_{HV}E_{HH}^* \rangle} = \exp\{j[2(\phi_H - \phi_V) + \overline{\delta_{VH}} \\ &\quad - \overline{\delta_{VV}} - \overline{\delta_{HV}} - \overline{\delta_{HH}}]\} \times \frac{\sum_i |S_{VH}^i|^2 |S_{VV}^i|^2}{\sum_i |S_{HV}^i|^2 |S_{HH}^i|^2} \end{aligned} \quad (27)$$

and

$$\arg(\mu) = 2(\phi_H - \phi_V) + \Delta, \quad (28)$$

where  $\Delta = \overline{\delta_{VH}} - \overline{\delta_{VV}}$  since  $\overline{\delta_{VH}} \approx \overline{\delta_{HV}}$ . [From the reciprocity theorem for scattered waves (e.g., Saxon, 1955)  $\delta_{VH}^i = \delta_{HV}^i$  identically. The approximate equality for the mean values in this instance arises from slight difference in the weighting factors when computing the means.] Often after only a rather short penetration into rain,  $2(\phi_H - \phi_V) \gg \Delta$  since  $\Delta$  will be small for Rayleigh-Gans scatterers. As a consequence the propagation differential phase shift may be estimated from

$$(\phi_H - \phi_V) \approx \frac{1}{2} \arg(\mu). \quad (29)$$

### 5. Estimation of $\Phi_{HV}$

The range rate of change of  $\Phi_H - \Phi_V$  must be estimated from measurements of the propagation differential phase shift at different locations along the direction of transmission. For discussion consider noise-free measurements made at range  $R_1$  and at a second range  $R_2 = R_1 + \Delta R$ . Then

$$\arg(\mu_2) - \arg(\mu_1) = 2[(\phi_H - \phi_V)_2 - (\phi_H - \phi_V)_1] + \Delta_2 - \Delta_1, \quad (30)$$

where the subscripts denote the two locations. The average range rate of differential phase shift over  $R$  is then estimated to be

$$\Phi_{HV}^m = \Phi_{HV}^t \left\{ 1 + \frac{\Delta_2 - \Delta_1}{2[(\phi_H - \phi_V)_2 - (\phi_H - \phi_V)_1]} \right\}, \quad (31)$$

where  $\Phi_{HV}^m$  denotes the expected value and  $\Phi_{HV}^t$  is the true mean value. Obviously  $\Phi_{HV}^m$  approaches  $\Phi_{HV}^t$  the smaller  $\Delta_2 - \Delta_1$  is with respect to the denominator which is simply the two-way total propagation differential phase shift over  $\Delta R$  (Fig. 3). The limits of  $\pm 0.2^\circ$  in Fig. 3 correspond to the extrema of  $\Delta_2 - \Delta_1$  that can be expected for horizontally oriented oblate water drops (see Jameson and Mueller, 1985) observed at a wavelength of 10.71 cm. Expression (31) of course represents an upper limit to the accuracy

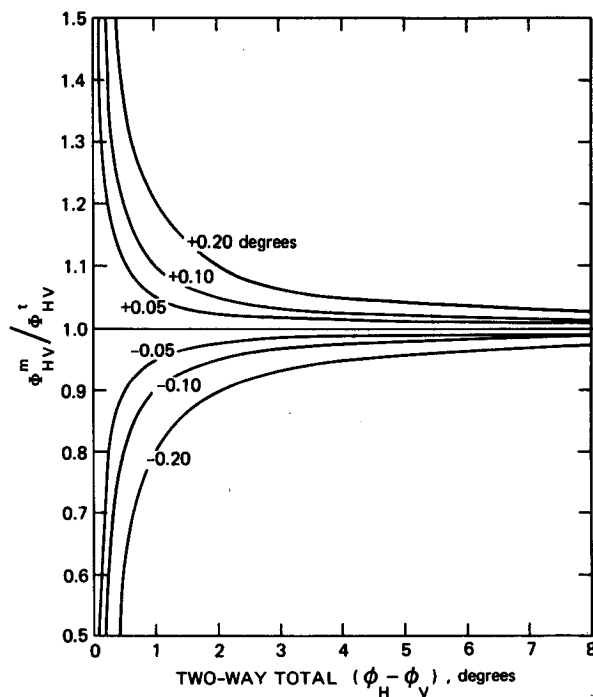


FIG. 3. The ratio of expected ( $\Phi_{HV}^m$ ) to the true ( $\Phi_{HV}^t$ ) rate of differential phase shift for  $\Delta_2 - \Delta_1$  between  $\pm 0.2^\circ$  as a function of total two-way differential phase shift over range increment  $\Delta R$ .

to which  $\Phi_{HV}$  can be determined since actual measurements would be affected by other factors such as system noise.

### 6. Discussion

For an ensemble of horizontally oriented quiescent oblate water drops, it has been shown (4b) that the range rate of propagation differential phase shift between horizontally and vertically polarized transmitted waves ( $\Phi_{HV}$ ) is proportional to the liquid water content ( $W$ ) times a shape factor  $(1 - \mathfrak{R})$  where  $\mathfrak{R}$  is the mass weighted mean axis ratio over the drop size distribution. Methods for estimating  $\mathfrak{R}$  and  $\Phi_{HV}$  have also been presented.

Although the intent of this paper is only to identify some of the meteorological factors which influence propagation differential phase shift, the obvious potential for estimating  $W$  warrants some discussion. The applicability of (4b) to natural rain will depend on the adequacy of the simple model of rain employed in the derivation. Strictly speaking the simple model is incorrect since almost all raindrop distributions will have some number of drops actively involved in the processes of collision, coalescence, and break-up. The question is not whether this active component exists but rather under what conditions the subsequent shapes, canting and possible oscillations of these drops will confound an interpretation of measurements based on (4b). Since so little is known quantitatively either about the proportion of the total number of drops involved in the various processes or of the resulting shapes and orientations of the active drops it seems likely that any potential application of (4b) will have to be evaluated experimentally in a variety of meteorological conditions. The relationship, however, does provide a convenient tool for at least some preliminary numerical simulations of propagation differential phase shift at long wavelengths in rain without having to refer to the complex scattering amplitude functions.

*Acknowledgment.* This work was supported by Grants NSF ATM 82-16847 and NSF ATM 83-18355 from the National Science Foundation.

### REFERENCES

- Beard, K. V., and A. R. Jameson, 1983: Raindrop canting. *J. Atmos. Sci.*, **40**, 448-454.
- Gans, R., 1912: Über die form ultramikroskopischer Goldteilchen. *Ann. Phys.*, **37**, 881-900.
- Hendry, A., and Y. M. M. Antar, 1984: The variation of echo cross-polarized echo intensity in rain with direction of polarization and its implication for canting angle distribution. *22nd Conf. Radar Meteorology*, Boston, Amer. Meteor. Soc., 382-386.
- Humphries, R. G., 1974: Observations and calculations of depolarization effects at 3 GHz due to precipitation. *J. Rech. Atmos.*, **8**, 155-161.

- Jameson, A. R., 1983a: Microphysical interpretation of multiparameter radar measurements in rain. Part I: Interpretation of polarization measurements and estimation of raindrop shapes. *J. Atmos. Sci.*, **40**, 1792-1802.
- , 1983b: Microphysical interpretation of multiparameter radar measurements in rain. Part II: Estimation of raindrop distribution parameters by combined dual-wavelength and polarization measurements. *J. Atmos. Sci.*, **40**, 1803-1813.
- , and E. A. Mueller, 1985: Estimation of differential phase shift from sequential orthogonal linear polarization radar measurements. *J. Atmos. Ocean. Technol.*, in press.
- Johnson, D. B., and K. V. Beard, 1984: Oscillation energies of colliding raindrops. *J. Atmos. Sci.*, **41**, 1235-1241.
- McCormick, G. C., and A. Hendry, 1974: Polarization properties of transmission through precipitation over a communication link. *J. Rech. Atmos.*, **8**, 175-187.
- , —, and B. L. Barge, 1972: The anisotropy of precipitation media. *Nature*, **238**, 214-216.
- Pruppacher, H. R., and R. L. Pitter, 1971: A semi-empirical determination of the shape of cloud and rain drops. *J. Atmos. Sci.*, **28**, 86-94.
- Saxon, D. S., 1955: Tensor scattering matrix for the electromagnetic field. *Phys. Rev.*, 1771-1775.
- Seliga, T. A., and V. N. Bringi, 1976: Potential use of radar differential reflectivity measurements at orthogonal polarizations for measuring precipitation. *J. Appl. Meteor.*, **15**, 69-76.
- Sinclair, G., 1948: Modification of the radar equation for arbitrary targets and arbitrary polarizations. Rep. No. 302-19, Antenna Laboratory, Ohio State University, Columbus.
- Ulbrich, C. W., 1983: Natural variations in the analytic form of the raindrop size distribution. *J. Climate Appl. Meteor.*, **22**, 1764-1775.
- van de Hulst, H. C., 1957: *Light Scattering by Small Particles*, Wiley and Sons, 470 pp.
- Warner, C., and A. Hizal, 1976: Scattering and depolarization of microwaves by spheroidal raindrops. *Radio Sci.*, **11**, 921-930.